DOI: 10.1002/((please add manuscript number))
Article type: Communication

A low cost desktop electrochemical metal 3D printer

*Xiaolong Chen[1], Xinhua Liu[1], Peter Childs[1], Nigel Brandon[2] and Billy Wu[1]**

[1] Dyson School of Design Engineering, Imperial College London, UK
[2] Department of Earth Science and Engineering, Imperial College London, UK
*e-mail of corresponding author: billy.wu@imperial.ac.uk

Additive manufacturing (AM)(3D printing) is the process of creating complex 3D geometries, through the layer-by-layer solidification of material, as opposed to traditional subtractive manufacturing methodologies.[1] The design freedom offered by the AM of metals has seen industrial uptake in aerospace[2], automotive[3] and medical[4] applications. Of the metal AM processes, direct metal laser sintering (DMLS) is the most common and works through the selective laser sintering of layers of metal powders.[1] Wider commercial uptake of metal AM is currently limited by the high capital cost, component defects[5] and inability to work with multiple materials. Thus, there is a need to develop novel non-laser based 3D printing techniques for metals which enable multiple materials to be deposited at reduced cost in order to unlock functional structures.

Electrochemical additive manufacturing (ECAM)(electrochemical 3D printing) is a relatively new form of AM that deposits thin and highly adherent layers of metal onto the surface of a conductive substrate through the reduction of metal ions in a solution.[6,7] There have been a number of different approaches taken to create an electrochemical 3D printer. Suryavanshi and Yu[8] fabricated individual copper nanowires via electrochemical deposition with a nano-pipette and achieved wire diameters of 200 nm and lengths of up to 10 µm. From the transmission electron microscopy (TEM) diffraction patterns of the printed wires, they showed that the deposition was polycrystalline, though it was suggested that by adjusting the deposition

conditions crystalline copper can be formed if the kinetics of the initial nuclei growth are faster than the formation of new nuclei. One challenge of this approach is that, at low operating humidity of <35 %, the copper sulphate crystallised out of solution due to the high evaporation rate near the pipette tip causing blockages. Suryavanshi and Yu limited their deposition potential to avoid the electrolysis of water and thus their deposition rates were relatively slow. They suggest that an increase in electrolyte concentration from 0.05 M would increase the current density and thus deposition rate however this would exasperate the blockage issue. They deposited at 0.4 V (between their copper electrode and gold/silicon substrate with no reference electrode) with a retraction speed of 0.25 $\mu m.s^{-1}$ which equates to a deposition rate of 0.008 $\mu m^3.s^{-1}$.

Hu and Yu[9] proposed a similar meniscus confined electrode (MCE) approach for creating copper wires. Electrochemical deposition of copper from copper sulphate was achieved at a potential of 0.2 V with a 0.05 M electrolyte concentration under ambient conditions. They showed that the retraction speed can be used to control the thickness of the wire through the narrowing of the meniscus. The challenges associated with the stability of the meniscus were highlighted since it is a function of the withdrawal speed, electrolyte and mechanical stability of the system, thus requiring a high degree of control. Hu and Yu limited their pipette size to 1.6 µm in diameter with a retraction speed between 0.3 $\mu m.s^{-1}$ and 0.6 $\mu m.s^{-1}$, to generate a wire diameter between 800 nm and 1,600 nm (Maximum deposition rate of 1.2 $\mu m^3.s^{-1}$). As a result, the deposition was relatively slow and the size of deposited copper was micron scale. To improve this, they suggested an increase in electrolyte concentration and pipette size, however this could change thermodynamic conditions of the interfacial forces at the three-phase region between the electrolyte, air and growing wire[9,10] which could result in an unstable meniscus.

Seol et al.[11] developed a simple strategy to improve the previous meniscus guided direct writing approaches through modulating the applied potential with different amplitudes and durations. Using this approach, a hollow micro tube was deposited by modulating the pulse potentials (2 V with a duty cycle of 33 %, with 0.8 V being applied during the rest cycle). This promoted preferential deposition at the meniscus edge. In order to obtain a solid structure, they added a negative etching step (-0.1 V) with the positive deposition potential (2 V) to suppress preferential deposition at the tip. With this approach, complex 3D metallic microarchitectures were achieved with a diameter of 12 μm equating to a deposition rate of 20.4 $\mu m^3.s^{-1}$ (0.18 $\mu m.s^{-1}$), with an electrolyte concentration of 1 M and relative humidity of 50 %.

Localised electrochemical deposition (LCD) is another ECAM approach which differs from the meniscus confined technique. It uses an ultra-sharp electrode submerged in an ionically conductive electrolyte close to a conductive substrate where the deposition occurs. A potential is applied between the tip and the substrate, which results in a localised deposition. [12] Said et al.[13] demonstrated the LCD technique in which they used a platinum wire encased in glass as their electrode. However, they highlighted the challenges in monitoring deposition currents and matching the retraction rate of the electrode to avoid short-circuiting. With the addition of laser based solution jetting to promote mass transport, the LCD method demonstrated deposition rates higher than the meniscus confined method of upto 10 $\mu m.s^{-1}$ for a 50 μm gold deposition (19,634 $\mu m^3.s^{-1}$). [14] The criticality of the inter-electrode gap for the LCD technique was highlighted in the numerical study by Kamaraj et al.[15] and Müller et al.[16] which discusses the interplay between diffusion controlled deposition and electric field migration. They suggested that too small a gap can result in inconsistent deposition through localised depletion of species.

Lin et al.[17] further investigated the influence of deposition parameters, such as potential and duty cycles, on the structure and surface morphologies of micro-scale copper columns. They showed that a higher voltage (3.2 V) with larger duty cycles (0.5) could lead to a column with a porous structure and rough surface finish compared to a lower deposition potential of 2.8 V with a duty cycle of 0.1 which exhibits dense features. More aspects have been discussed by other researchers. Heβ et al.[18] focused on non-conducting substrate deposition. Yeo et al.[19] improved the deposition morphology and deposition speeds via a rotating electrode. In further research, Yeo et al.[20] investigated the use of ultrasonic vibration with the LCD technique and showed that concentricity of the printed wires improved but at the cost of increased porosity. Other influencing factors such as resolution, complexity of geometries, repeatability, deposition mechanism and integration were investigated by Said et al. [13,21]

To date, all of the presented ECAM methods (LCD and MCE) are designed to achieve micro or nano scale structures using expensive piezo-based movement stages and nano-pippettes/ultra-fine electrodes. Limited deposition rates for copper based systems ranging from ~100 $nm.s^{-1}$ to ~0.18 $\mu m.s^{-1}$ (0.008-20.4 $\mu m^3.s^{-1}$) remains the main barrier to upscaling and competing against conventional 3D printing methods such as DMLS. Furthermore, all the printed structures are of limited geometry complexities, with the majority being wire-based architectures with often porous and rough morphologies and limited characterisation of the properties of the printed structures. Thus, there is a need to develop larger ECAM systems with improved deposition rates capable of printing more complex structures than linearly extruded micro-scale objects. Here, we report a novel and simple strategy for ECAM using a MCE approach but at a significantly larger scale, with a 400 µm nozzle (equivalent to plastic 3D printing). This work provides a systematic overview of factors which influence the speed of deposition and also how this influences product morphology and physical properties such as

hardness and electrical resistivity laying the foundations for the development of a low-cost desktop electrochemical 3D printer. Whilst, the initial work focuses on the electrodeposition of copper from aqueous copper sulphate, this can be transferrable to other chemistries.

Figure 1a-Figure 1c shows a schematic of the electrochemical 3D printer. A plastic syringe and nozzle (diameter 400 µm) with an open pore sponge is filled with a solution of copper sulphate. The porous sponge is inert to the electrolyte and serves the purpose of providing sufficient back pressure to the hydraulic head such that a stable meniscus can be formed. Without this sponge, the electrolyte readily flows through the large nozzle since the surface tension of the electrolyte cannot maintain the meniscus. Detailed information about the rig design is provided in the supplementary information. The nozzle/syringe assembly (print head) is mounted on a carriage that can be moved in the x and y direction, with the stationary platform also able to move in the z direction through the use of computer controlled stepper motors. Two copper rods are suspended in the copper sulphate electrolyte and act as a counter and reference electrode. The reference electrode is used to correct for polarisation overpotentials during the deposition process. A working and sense electrode is connected to a copper substrate plate. To create a structure, the print head contacts the copper substrate and retracts a small amount to form a stable meniscus. A positive potential is then applied between the working and counter electrodes to deposit copper onto the substrate through the reduction of Cu^{2+} ions. The Cu^{2+} ions are simultaneously replenished from the counter electrode through the accompanying oxidation reaction to form a concentration gradient controlled through a combination of diffusion and migration. The print head is then moved in the x and y directions as defined by the tool path generated based on the 3D computer model. **Figure 1d** shows an optical image of the printed letters “ICL” using a deposition potential of 5 V vs Cu, with a 1 M

$CuSO_4$ concentration and print head speed of 0.4 $mm.s^{-1}$. All printed letters were removed from the base plate and placed onto scanning electron microscopy (SEM) stubs with carbon tape.

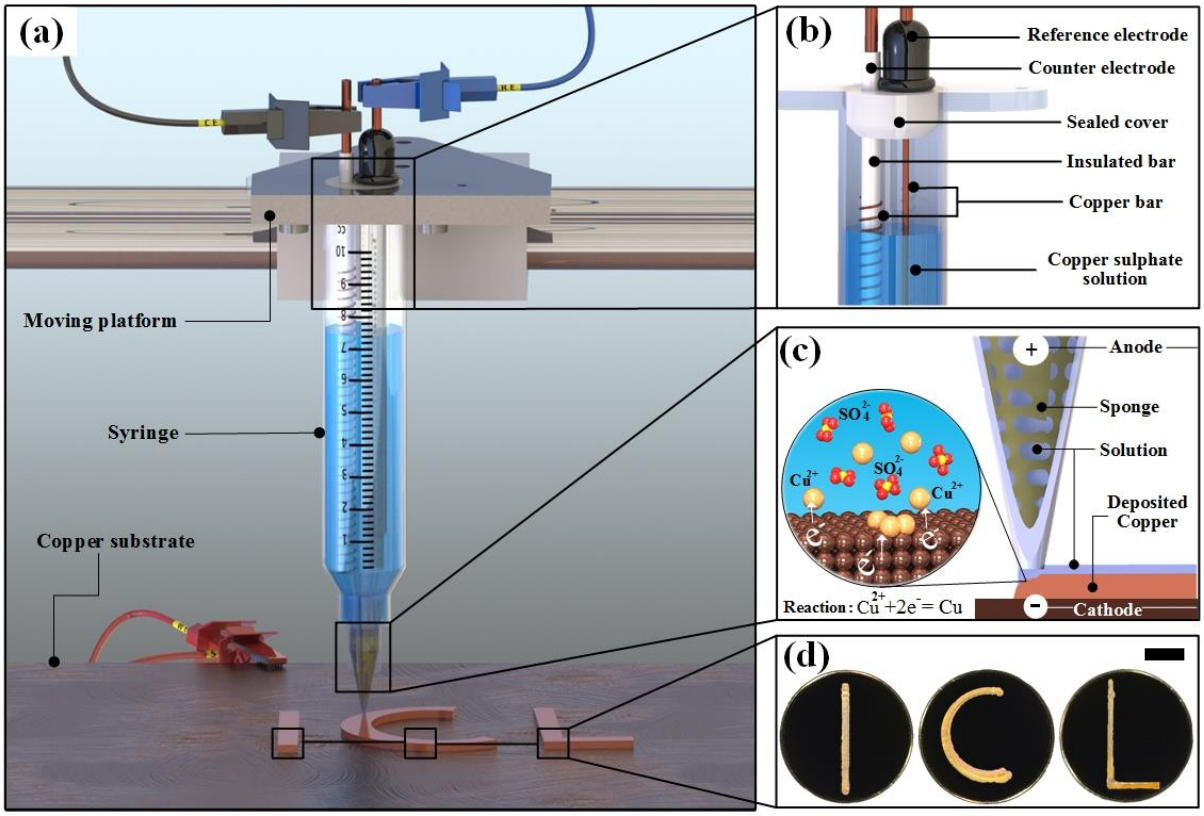

Figure 1: Schematic illustration of the electrochemical 3D printer. a) Overview of print head set-up. b) Detail view illustrating electrode arrangement. c) Detailed view of the print nozzle highlighting the copper deposition process and the sponge in the tip. d) Optical images of the printed copper structures featuring the letters "ICL". The scale bar represents 2mm in length.

Fabrication of dots and lines were performed using a copper sulphate concentration of 1 M with deposition voltages ranging from 1 V-6 V vs Cu under ambient conditions. **Figure 2** shows the SEM micrographs of the printed dots with a deposition time of 1 hour with details of the SEM conditions provided in the supplementary material. Of the samples, the 1 V deposition exhibited the most ideal morphology, with a dense structure and high degree of concentricity due to the meniscus confinement approach. The 2 V vs Cu sample showed a faster rate of growth with a dense structure, however exhibited a convex shape due to preferential deposition at the centre. At 3 V vs Cu, the formation of copper dendrites becomes apparent due to mass transport limitations with the severity and porosity continuing to increase with

increasing deposition potential. At 4 V vs Cu, the base of the deposition becomes dendritic also but with a finer morphology compared to higher regions. The switch between fine and course dendritic structures between the base and upper regions of the dots suggest that there is a shift in the deposition conditions which may arise due to the interplay between diffusion and migration, as well as different nucleation kinetics on the neat copper substrate vs a copper dendrite. The SEM images suggest all samples are polycrystalline with a decreasing grain size with increasing deposition potential suggesting there is a shift in the physical properties. Further SEM and optical images are provided in the Supplementary material in **Figures S1-S10**). The current density for the various depositions are shown in **Figure S11**. Whilst deposition speed naturally increases with a higher potential, the morphology due to mass transport limitations beyond 2 V vs Cu needs to be addressed in order to achieve dimensionally accurate structures.

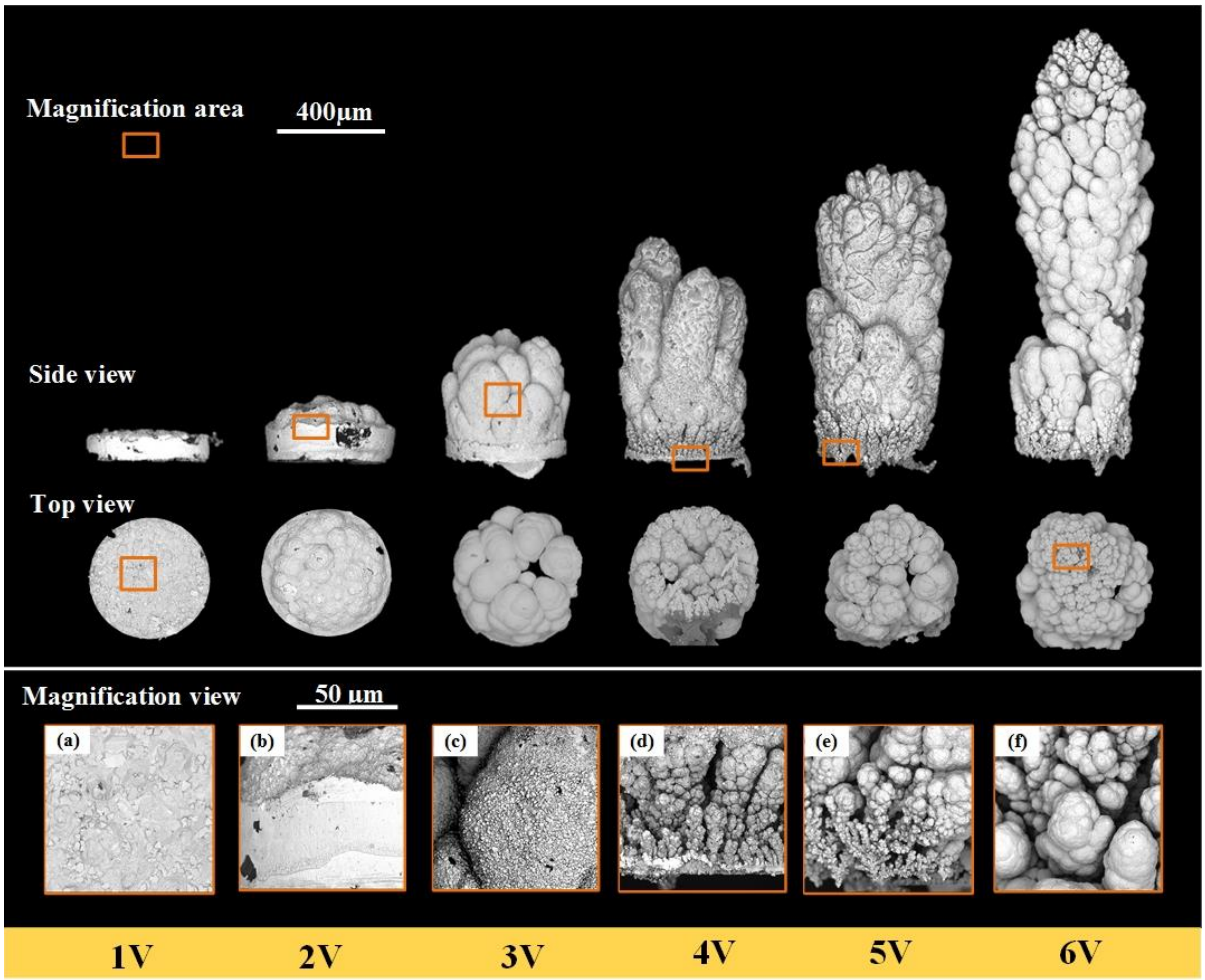

Figure 2: SEM images of single dot copper depositions at different potentials

Figure 3 shows the SEM micrographs of the printed structures now with a lateral print head velocity of 0.4 $mm.s^{-1}$ and the same deposition conditions of 1 M $CuSO_4$ and ambient conditions over a potential range of 1 V-6 V vs Cu. The formation of pure elemental copper was confirmed through energy dispersive x-ray spectroscopy (EDS) measurements (**Figure S12**). Of note is the fact that the deposition morphology is no longer dendritic suggesting that the relative position of the print head aids with mass transport of copper ions or mechanical removal of the dendrites. For a 1 hour deposition it can be observed that the line thickness increases from 3 µm at 1 V vs Cu to a peak of 15 µm at 4 V vs Cu after which there is a decrease in deposited material, due to falling deposition efficiency. Given the lateral speed at 0.4 $mm.s^{-1}$ over a distance of 10 mm and time of 3600 s, this suggests that 144 passes were made. From Figure 3, the line thicknesses ranged from 3-15 µm, which suggests a layer thickness of 14-104 nm. This is confirmed from the striations observed in the magnified view of the 5 V vs Cu deposition. This suggests that the z-height resolution of this process is exceptionally high and opens the possibility of this technique in the fabrication of functional electronics such as sensors.

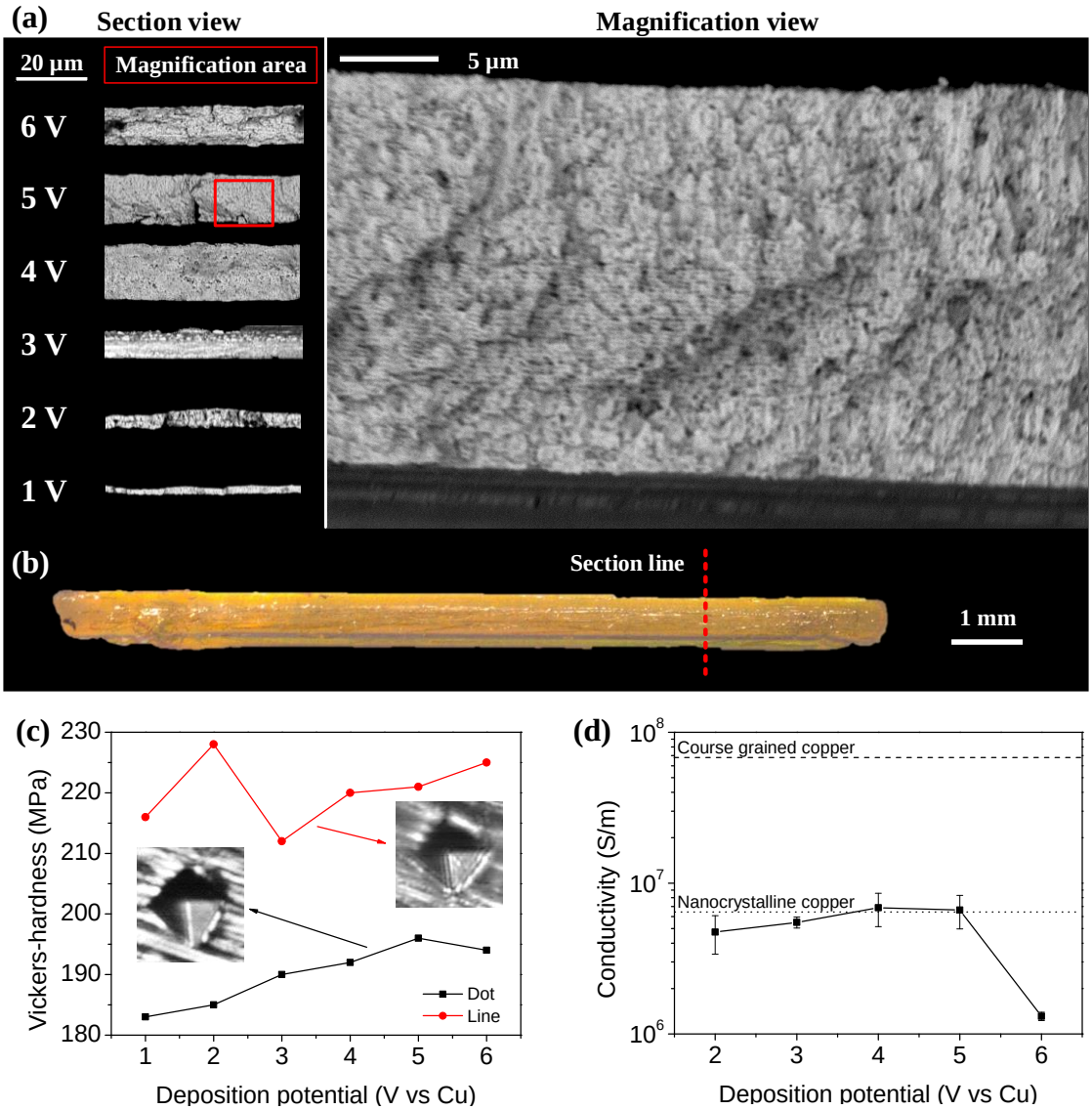

Figure 3: (a) SEM images of cross section of line depositions and a magnified view of the 5V deposition showing striations due to the printing process. (b) An optical image of the 5V printed line. (c) Vickers-hardness measurements of the printed lines and dots. (d) Electrical conductivity measurements of the printed lines.

The highly polycrystalline nature of the printed structures suggest that the mechanical properties of the printed structures deviate from conventional cold worked cast copper. **Figure 3c** shows the Vickers hardness of the copper dots and lines. For a single dot, the hardness ranges from 184-196 MPa with values increasing with deposition potential most likely due to the decreasing grain size. The Vickers hardness of the printed line exhibited even higher values ranging from 211-228 MPa, likely due to even further smaller grains due to the mechanical agitation increasing the rate of deposition as observed in **Figure S11**. As a reference, the hardness of copper used in circuit bonding wires can range from 50 to 176 MPa.[22]

Figure 3d demonstrates the result of the conductivity measurements of single lines via a four probe apparatus. Here the electrical conductivity of samples were found to range between $1.31x10^6$ and $6.86x10^6$ S/m. This is broadly 1 order of magnitude below the conductivity of course grained copper ($5.92x10^7$ S/m) reported by Lu et al.[23] but agrees well for nanocrystalline copper ($5.41x10^6$ S/m) measurements supporting the observation that the electrodeposition of copper results in highly nanoycrystalline structures.

The work presented demonstrates that large scale (400 µm nozzle) meniscus confined electrochemical printing is possible through the novel printer design proposed. This concept balances the hydraulic head of a static electrolyte with the back pressure of a sponge filled nozzle to form a stable meniscus. Static printing of copper dots from a 1 M $CuSO_4$ solution gives dense prints at low voltages of 1 V vs Cu however at increasing voltages >3 V vs $CuSO_4$ there is an evident evolution of dendritic structures due to the diffusion limitations of the Cu^{2+} ions. The novel concept of print head movement, has been shown to suppress dendrite formation, likely due to the mechanical agitation of the electrolyte through entrainment effects. This thus, enables a faster rate of deposition of upto 19,667 $\mu m^3.s^{-1}$ without noticeable dendritic formations. This is 3 orders of magnitude faster than previously reported copper deposition studies (20.4 $\mu m^3.s^{-1}$) opening the possibility for the printing of larger structures. Printed structures had a noticeable polycrystalline grain structure, with decreasing grain size with increasing deposition potential. Mechanical and electrical characterisation, show that the Vickers hardness and electrical resistivity are higher than cold worked cast copper due to the fine grain structure. This work therefore builds a foundation for future work on high speed and low cost ECAM with expanding research areas such as multi-material functional structures.

Experimental section

The electrochemical 3D printer is based on a modified WER Me Creator fused deposition modelling 3D printer with the hot end replaced with a carriage holding a 10 mL polypropylene dispensing syringe (Metcal-7100LL1NPK) with a 400 μm polypropylene needle (Metcal-922125-DHUV). Copper sulphate electrolytes were prepared by mixing anhydrous copper (II) sulphate (≥99.99% pure – Sigma Aldrich) with deionised water. Deposition and electrical conductivity measurements were conducted using a Metrohm Autolab PGSTA302N in a 4-electrode configuration. Hardness measurements were conducted using a Zwick-ZHV1 micro Vickers hardness machine. Silicon carbide paper with a grade of 1500 was used to polish all samples before epoxy mounting. During the experiments, a minimum load of 10 gmf was applied to all samples with creep time of 10 seconds. SEM images were taken with a Phenom ProX in backscattered mode with an acceleration voltage of 5 kV with no sample sputtering.

Supporting information

Supporting Information is available from the Wiley Online Library or from the author.

Acknowledgments

This research was financially supported by the Chinese Scholarship Council for Xiaolong Chen and the EPSRC Joint UK India Centre for Clean Energy (EP/P003605/1) and Energy Storage for Low Carbon Grids (EP/K002252/1) project for Xinhua Liu.

References

[1] W. E. Frazier, *J. Mater. Eng. Perform.* **2014**, *23*, 1917.

[2] G. D. Goh, S. Agarwala, G. L. Goh, V. Dikshit, S. L. Sing, W. Y. Yeong, *Aerosp. Sci. Technol.* **2017**, *63*, 140.

[3] N. Guo, M. C. Leu, *Front. Mech. Eng.* **2013**, *8*, 215.

[4] X. Wang, S. Xu, S. Zhou, W. Xu, M. Leary, P. Choong, M. Qian, M. Brandt, Y. M. Xie, *Biomaterials* **2016**, *83*, 127.

[5] K. A. Ibrahim, B. Wu, N. P. Brandon, *Mater. Des.* **2016**, *106*, 51.

[6] M. Paunovic, M. Schlesinger, John Wiley & Sons., *Fundamentals of Electrochemical Deposition*, Wiley, **2006**.

[7] M. M. Sundaram, A. B. Kamaraj, V. S. Kumar, *J. Manuf. Sci. Eng.* **2015**, *137*, 21006.

[8] A. P. Suryavanshi, M.-F. Yu, *Appl. Phys. Lett.* **2006**, *88*, 83103.

[9] J. Hu, M.-F. Yu, *Science (80-.).* **2010**, *329*, 313.

[10] J. Eastoe, J. S. Dalton, *Adv. Colloid Interface Sci.* **2000**, *85*, 103.

[11] S. K. Seol, D. Kim, S. Lee, J. H. Kim, W. S. Chang, J. T. Kim, *Small* **2015**, *11*, 3896.

[12] J. D. Madden, I. W. Hunter, *J. Microelectromechanical Syst.* **1996**, *5*, 24.

[13] R. A. Said, *Nanotechnology* **2004**, *15*, S649.

[14] M. H. Gelchinski, L. T. Romankiw, D. R. Vigliotti, R. J. VON Gutfeld, **1985**.

[15] A. Kamaraj, S. Lewis, M. Sundaram, *Procedia CIRP* **2016**, *42*, 788.

[16] A. D. Müller, F. Müller, M. Hietschold, *Thin Solid Films* **2000**, *366*, 32.

[17] J. C. Lin, T. K. Chang, J. H. Yang, Y. S. Chen, C. L. Chuang, *Electrochim. Acta* **2010**, *55*, 1888.

[18] C. Heβ, K. Borgwarth, C. Ricken, D. G. Ebling, J. Heinze, *Electrochim. Acta* **1997**, *42*, 3065.

[19] S. H. Yeo, J. H. Choo, *J. Micromechanics Microengineering* **2001**, *11*, 435.

[20] S. H. Yeo, J. H. Choo, K. H. A. Sim, *J. Micromechanics Microengineering* **2002**, *12*, 271.

[21] R. A. Said, *Nanotechnology* **2003**, *14*, 523.

[22] J. Yeung, L. C. Keong, *Procedia Eng.* **2014**, *75*, 134.

[23] L. Lu, Y. Shen, X. Chen, L. Qian, K. Lu, *Science (80-.).* **2004**, *304*, 422.